



1 **Multi-Decadal Expansion of Potentially Dangerous Glacial**  
2 **Lakes in Central-Eastern Nepal (1992-2024): Remote Sensing**  
3 **Assessment and GLOF Hazard Implications**  
4

5 Ashok Ghimire<sup>1</sup>, Susa Manandhar<sup>1</sup>, Tribikram Basnet<sup>1</sup>, Kumar Aryal<sup>1,2</sup>, Sushant Dhital<sup>1</sup>,  
6 Reshu, Karki<sup>1</sup>, Aakriti Dhakal<sup>1</sup>, Nir Krakauer<sup>3</sup>, Dhiraj Pradhananga<sup>1,2</sup>  
7

8 <sup>1</sup>The Small Earth Nepal, Kathmandu, Nepal

9 <sup>2</sup>Department of Meteorology, Tri-Chandra Multiple Campus, Tribhuvan University, Kathmandu, Nepal

10 <sup>3</sup>Department of Civil Engineering, City College of New York, USA  
11

12 *Correspondence to:* Dhiraj Pradhananga (dhiraj.pradhananga@trc.tu.edu.np)  
13

14 **Abstract.** Glacial lakes in the Himalayan regions are expanding rapidly under ongoing climate change,  
15 intensifying the risk of Glacial Lake Outburst Floods (GLOFs). This study quantifies multi-decadal area changes  
16 (1992-2024) in four Potentially Dangerous Glacial Lakes (PDGLs), Thulagi, Lumding Tsho, Hongu 2, and Lower  
17 Barun, located in central-eastern Nepal, using Landsat 5 and Landsat 8 satellite imagery processed within the  
18 Google Earth Engine (GEE) cloud platform. Lake boundaries were delineated from post-monsoon (October-  
19 November) median composites using the Normalized Difference Water Index (NDWI; threshold = 0.3),  
20 supplemented by manual delineation where topographic shadow conditions compromised automated extractions.  
21 Area uncertainties were computed using the standard half-pixel buffer method. Non-parametric Mann-Kendall  
22 trend tests with Sen's slope estimator were applied to all lake area time series to evaluate the statistical significance  
23 and rate of expansion. Sub-period regression analysis was used to assess acceleration in lake growth. Empirical  
24 area-volume scaling was applied to estimate changes in impounded water volume. All four lakes exhibited  
25 statistically significant, monotonically increasing area trends over the 32-year study period (Mann-Kendall tau =  
26 1,  $p < 0.001$  for each lake). Lower Barun exhibited the highest expansion rate (Sen's slope =  $0.063 \text{ km}^2 \text{ yr}^{-1}$ ),  
27 growing from  $0.77 \pm 0.053 \text{ km}^2$  in 1992 to  $2.76 \pm 0.13 \text{ km}^2$  in 2024 (a 258% increase), with post-2010 expansion  
28 accelerating by a factor of 1.35. Lumding Tsho showed a strongly accelerating growth trajectory ( $R^2 = 0.96$ ) with  
29 a post-2010 rate that more than doubled. The combined estimated additional water volume stored across all four  
30 lakes since 1992 approaches  $608.6 \times 10^6 \text{ m}^3$ , representing a GLOF hazard of exceptional and growing scale. The  
31 approach demonstrates a scalable and reproducible framework for long-term glacial lake monitoring and hazard  
32 assessment, applicable across data-sparse high mountain environment.  
33

34 *Keywords:* Glacial lakes, Thulagi, Lumding Tsho, Hongu 2, Lower Barun, Google Earth Engine  
35

36 **1 Introduction**  
37

38 The cryosphere of the Himalayas is undergoing accelerated transformation under anthropogenic climate change.  
39 Globally, glacial lake volume and area increased by approximately 48% and 51% respectively from 1990 to 2018,  
40 representing one of the most dramatic landscape-scale responses to warming documented in the satellite era  
41 (Shugar et al., 2020). Even if global temperatures were stabilised today, glaciers would continue to lose mass for  
42 several decades due to the long adjustment time of the cryosphere to climate change (Lee & Romero, 2023),



43 ensuring that proglacial lakes will continue forming and expanding regardless of near-term mitigation efforts. The  
44 region is particularly exposed to these changes: its complex topography, steep elevation gradients, and strong  
45 orographic controls create conditions in which small climatic perturbations can trigger large geomorphological  
46 responses (Bajracharya et al., 2015).

47

48 Glacier extent in the Himalayan region is the largest outside the polar regions, supporting freshwater resources  
49 for approximately 2 billion people at risk of water stress across South and Southeast Asia. However, accelerated  
50 glacier mass loss; estimated at 65% in the HKH region over recent decades, is fundamentally altering the  
51 hydrological regimes of downstream river systems (ICIMOD, 2023). As glaciers retreat, they expose over-  
52 deepened bedrock basins or leave behind moraine-dammed depressions that fill with meltwater, forming  
53 proglacial lakes. These lakes grow as their parent glaciers retreat further, accumulating enormous volumes of  
54 water behind naturally unstable ice-cored or debris moraine dams. A sudden failure of these dams, whether  
55 triggered by ice calving, seismic activity, extreme precipitation, or slope instability, can release catastrophic  
56 outburst floods that sweep through steep valley systems with a little warming, threatening communities,  
57 infrastructure, and hydropower assets many kilometres downstream (Duan et al., 2023; Shugar et al., 2020).

58

59 Nepal is among the most GLOF-exposed nations on Earth. With 47 Potentially Dangerous Glacial Lakes (PDGLs)  
60 identified, of which 21 lie entirely within Nepal's borders, the country faces a disproportionate share of global  
61 GLOF risk (ICIMOD, 2011). Recent inventories document the scale of change: from 2000 to 2020, 499 new  
62 glacial lakes formed in Nepal, 139 vanished, and the net increase in lake area reached 19.46 km<sup>2</sup> with an additional  
63 403.07 × 10<sup>6</sup> m<sup>3</sup> of impounded water (Hu et al., 2022). In the broader Hindukush-Karakoram region, glacial lake  
64 numbers increased by 9.31% and total area expanded by 10.09% between 1990 and 2010 alone (Kumar et al.,  
65 2025). These aggregate statistics, however, obscure the site-specific dynamics that are essential for hazard-  
66 targeted risk management.

67

68 Among Nepal's most hazardous lakes, Thulagi, Lower Barun, Lumding Tsho, and Hongu 2 have been consistently  
69 identified in GLOF hazard assessments as warranting priority attention (Bajracharya et al., 2020; Chen et al.,  
70 2025). Thulagi is directly upstream of existing hydropower infrastructure; Lower Barun has undergone explosive  
71 growth driven by continuous calving from a debris-covered glacier and poses cascade flood risk to areas  
72 downstream (Gantayat et al., 2024; Maskey et al., 2020); Lumding Tsho has a short moraine dam adjacent to steep  
73 hanging ice (Bajracharya et al., 2020); and Hongu 2 is part of a cluster of rapidly evolving lakes in the Hongu  
74 Valley (Byers et al., 2013; Komori, 2006). Recognising this hazard profile, all four lakes have been selected under  
75 a Green Climate Fund (GCF)-supported initiative for lake lowering and ecosystem-based stabilisation (UNDP,  
76 2025).

77

78 Previous remote sensing studies have examined subsets of these lakes, notably Haritashya et al. (2018) for Thulagi  
79 and Lower Barun using multi-decadal Landsat data, and Gantayat et al. (2024) for the evolution of Lower Barun  
80 specifically, providing valuable insights into glacial lake distribution and change. However, several high-risk  
81 lakes, including Lumding Tsho and Hongu 2 remain comparatively under-represented in detailed long-term  
82 analyses. Existing studies often focus on individual sites or short time periods, lack methodological consistency,



83 and rarely quantify uncertainties or assess non-linear growth dynamics such as acceleration (Bajracharya et al.,  
84 2020; Gantayat et al., 2024; Maskey et al., 2020). As a result, there is limited understanding of how rapidly these  
85 potentially dangerous lakes are evolving and whether their expansion is intensifying over time. Addressing this  
86 gap is essential for developing robust, comparable, and process-informed assessments of glacial lake hazards.

87

88 This study therefore aims to: (i) quantify multi-decadal area changes and associated uncertainties for selected  
89 high-risk glacial lakes using a consistent Landsat-based framework; (ii) characterise the temporal dynamics, and  
90 non-linear growth behaviour including potential acceleration; (iii) estimate changes in stored water volume using  
91 empirical scaling relationships; and (iv) evaluate implications for evolving GLOF hazards in glacierized mountain  
92 regions.

93

## 94 **2 Study Area**

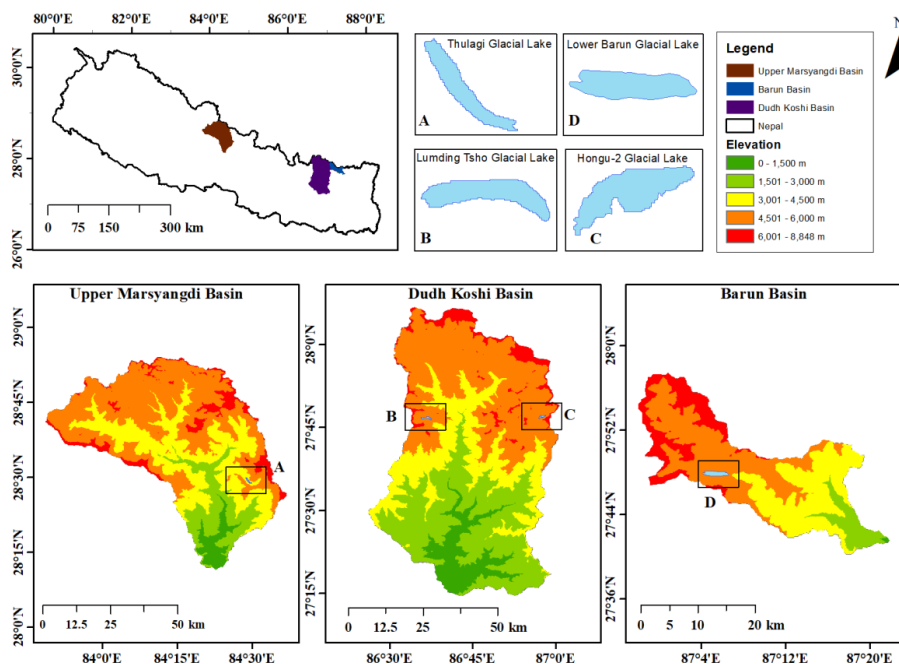
95

96 The study area encompasses three adjacent Himalayan sub-catchments in central-eastern Nepal: the Upper  
97 Marsyangdi (Thulagi), the Dudh Koshi (Lumding Tsho and Hongu 2), and the Barun (Lower Barun) basins. Each  
98 span steep altitudinal gradients from subtropical/temperate mid-hills to high alpine and nival zones where glacier  
99 and moraine-dammed lakes have developed (Bajracharya et al., 2020; Bocchiola et al., 2020; Sigdel et al., 2022).

100 The regional hydroclimate is dominated by the South Asian summer monsoon, which delivers approximately 70%  
101 of annual precipitation between June and September, creating a pronounced wet season contrasted with cold, dry  
102 winters (Bocchiola et al., 2020; Mudbhari et al., 2022; Pepin et al., 2022). These characteristics make the basins  
103 highly sensitive to changes in monsoon intensity, snowmelt timing, and glacier mass balance, jointly controlling  
104 seasonal streamflow, sediment delivery, and the likelihood of hydro-geomorphic hazard events (Bookhagen &  
105 Burbank, 2010; Neupane et al., 2015).

106

107 Figure 1 shows the locations of the three sub-catchments and the four study lakes.



108

109 **Figure 1: Three Himalayan sub-catchments, Upper Marsyangdi, Dudh Koshi, and Barun Basin, showing**  
 110 **the locations of the four study lakes**

111

112 **2.1 Upper Marsyangdi and Thulagi Glacial Lake**

113

114 The upper Marsyangdi sub-basin contains extensive debris-covered glaciers and several moraine-dammed  
 115 proglacial lakes fed by glacier melt and avalanche input from high ridges (Bajracharya et al., 2020). Mean annual  
 116 precipitation is highly variable with elevation, ranging from approximately 400 mm yr<sup>-1</sup> at the highest and most  
 117 arid sites to over 3200 mm yr<sup>-1</sup> at lower, wind-exposed slopes, with the bulk falling during the monsoon season  
 118 (Mudbhari et al., 2022).

119

120 Thulagi glacial lake is a moraine-dammed proglacial lake at the terminus of Thulagi glacier in the Upper  
 121 Marsyangdi region, situated at approximately 4,050 m a.s.l. Bathymetric surveys have documented a maximum  
 122 depth of approximately 76 m and an estimated volume of  $36.1 \times 10^6 \text{ m}^3$  (Haritashya et al., 2018). A breach of the  
 123 moraine dam would have direct downstream consequences for existing hydropower facilities and downstream  
 124 communities in the Marsyangdi valley.

125

126 **2.2 Dudh Koshi: Lumding Tsho and Hongu 2**

127

128 The Dudh Koshi sub-basin drains the southern flanks of the Everest-Makalu arc, spanning the full Himalayan  
 129 elevation range from approximately 500 m to 8,848 m, and contains numerous glacier termini and proglacial lakes  
 130 that modulate seasonal discharge (Nepal, 2016). Observed temperature and precipitation trends suggest warming



131 and increasing extreme precipitation frequency, with direct implications for glacier mass balance, lake expansion,  
132 and downstream flood risk (Bocchiola et al., 2020)

133

134 Lumding Tsho is a proglacial lake formed at the terminus of Lumding glacier at an elevation of approximately  
135 4,846 m a.s.l. (Ives et al., 2010). It is situated at approximately 27° 46' 59" N, 86° 57' 25" E, where steep slopes,  
136 nearby hanging glacier ice, and relatively short moraine dam contribute to a high monitoring priority ranking  
137 (Bajracharya et al., 2020; Chen et al., 2024). Remote sensing inventories have consistently listed Lumding Tsho  
138 among the lakes with the most rapid areal increases in Nepal (Hu et al., 2022).

139

140 Hongu 2 is located at the Hongu valley, a part of a cluster of actively evolving glacial lakes in the Makalu-Barun  
141 region. Historical records indicate that glacier termini in the Hinku and Hongu valleys have been retreating at  
142 approximately 70 m yr<sup>-1</sup> since the 1950s-1970s (Komori, 2006), and a neighbouring lake, Chamlang South Pokhari  
143 has been expanding at a rate of 0.117 km<sup>2</sup> yr<sup>-1</sup> from 1964 to 2010 (Byers et al., 2013), providing regional context  
144 for the rapid dynamics observed at Hongu 2.

145

### 146 **2.3 Barun and Lower Barun Glacial Lake**

147

148 The Barun sub-basin is located east of the Everest region within Makalu-Barun National Park. It contains the  
149 largest moraine-dammed lakes and most extensive debris-covered glaciers in eastern Nepal.

150

151 Lower Barun glacial lake lies in eastern Nepal's Mahalangur Himalaya at approximately 4,550 m a.s.l., close to  
152 the Makalu Massif (Gurung et al., 2021; Haritashya et al., 2018). It is dammed by an ice-cored moraine to the east  
153 and fed by a debris-covered glacier to the west, which continuously supplies icebergs through calving. Field  
154 measurements indicate a maximum depth of approximately 205 m and a volume of approximately  $112.3 \times 10^6$   
155 m<sup>3</sup>, making it one of the deepest and most voluminous lakes in the Nepal Himalaya. It faces compound hazard  
156 risks from rock and ice avalanches on nearby steep slopes and potential cascade GLOF scenarios (Maskey et al.,  
157 2020).

158

## 159 **3 Data and Methodology**

160

### 161 **3.1 Data Sources**

162

163 Landsat 5 Thematic Mapper and Landsat 8 Operational Land Manager (OLI) imagery at 30 m spatial resolution  
164 were accessed via Google Earth Engine (GEE) (Williams et al., 2006). The study period spans 1992-2024. Landsat  
165 7 ETM+ was deliberately excluded because the Scan Line Corrector (SLC-off) failure in May 2003 produced  
166 systematic data gaps of approximately 22% per scene (Scaramuzza et al., 2004), which would introduce artificial  
167 discontinuities in long-term boundary extraction. All imagery was accessed as Top of Atmosphere (TOA)  
168 reflectance. Post-monsoon periods (October-November) were selected for each year to minimize cloud cover and  
169 seasonal snowpack interference on lake delineation (Wangchuk & Bolch, 2020). Imagery was restricted to less  
170 than 20% cloud cover, and annual post-monsoon median composites were generated to further reduce cloud and  
171 shadow effects (Hermosilla et al., 2023; Jin et al., 2023). Annual composites were calculated at four-year intervals



172 from 1992; where suitable imagery was unavailable (2012-2013), the nearest available alternative year (2014)  
173 was substituted.

174

### 175 **3.2 Glacial Lake Delineation and Area Extraction**

176

177 Lake boundaries were delineated from post-monsoon Landsat median composites using the Normalized  
178 Difference Water Index (NDWI):

179

$$180 \quad NDWI = \frac{(Green - NIR)}{(Green + NIR)} \quad (1)$$

181 where, NIR is Near Infrared band

182

183 A pixel threshold of 0.3 (Gu et al., 2007; McFeeters, 2013) was applied to classify water pixels. All pixel areas  
184 meeting the threshold were summed to estimate annual lake area in km<sup>2</sup>. For scenes where accurate automatic  
185 delineation was compromised by topographic shadow effects on NDWI, particularly in narrow glacially-scoured  
186 valleys, GIS-based manual delineation was applied. For validation, Sentinel-2 imagery at 10 m spatial resolution  
187 (available from 2017 onwards) was used to independently delineate lake boundaries for the 2024 epoch, providing  
188 cross-sensor accuracy assessment of the Landsat NDWI-derived boundaries for the most recent time step  
189 (Wangchuk & Bolch, 2020).

190

### 191 **3.3 Area Uncertainty Quantification**

192

193 Mapping uncertainty for Landsat derived lake areas was quantified using the half-pixel buffer method (Fujita et  
194 al., 2009; Paul et al., 2013; Rounce et al., 2017).

195

$$196 \quad \Delta A = \frac{p}{2} \times L \quad (2)$$

197

198 where  $p$  is the pixel size (30 m) and  $L$  is the lake perimeter (m). Perimeter lengths were extracted from the GIS-  
199 delineated lake polygons for each time step. Representative uncertainty values for the 1992 and 2024 epochs are  
200 presented in Table 1.

201

### 202 **3.4 Volume Estimation**

203

204 The empirical area-volume (A-V) power-law scaling relationship of Cook & Quincey (2015) was applied:

205

$$206 \quad V = 0.104 \times A^{1.42} \quad (3)$$

207

208 where  $V$  is the estimated lake volume (km<sup>3</sup>) and  $A$  is the lake surface area (km<sup>2</sup>). This relationship was developed  
209 from a global compilation of glacial lake bathymetry data (Huggel et al., 2002) and has been widely applied for  
210 preliminary volume assessment in the Himalayas (Cook & Quincey, 2015; Shugar et al., 2020). Volume estimates



211 are reported as order-of-magnitude indicators, and for lakes where field measurements exist (Thulagi and Lower  
212 Barun), the scaling estimates are compared against field data to calibrate interpretation.

213

214 **3.5 Statistical Analysis**

215

216 **3.5.1 Mann-Kendall trend test and Sen’s slope**

217

218 The non-parametric Mann-Kendall (MK) trend test was applied to all lake area time series to evaluate the  
219 statistical significance of trends without assuming a normal distribution (Kendall & George, 1990; Mann, 1945).

220 The MK test is recommended for cryospheric time series because it is robust to non-normality, outliers, and  
221 missing values (Yue et al., 2002). Sen’s slope estimator was used as the trend magnitude estimator (Sen, 1968).

222 Both tests were conducted at the 95% confidence level.

223

224 The MK test statistic S is:

225 
$$S = \sum_{k=1}^{n-1} \sum_{j=k+1}^n \text{sgn}(x_j - x_k) \tag{4}$$

226 with variance,

227 
$$\text{Var}(S) = \frac{n(n-1)(2n+5)}{18} \tag{5}$$

228 where.....

229 The standardized test statistic Z was used to test the hypothesis of no trend at  $p < 0.05$ .

230

231 **3.5.2 Sub-period trend analysis**

232

233 To quantify post-2010 acceleration in lake expansion, linear regression was performed separately for the 1992-  
234 2010 and 2010-2024 sub-periods for each lake, and the ratio of sub-period slopes was calculated as the  
235 acceleration factor.

236

237 **4 Results**

238

239 **4.1 Glacial Lake Area Change (1992-2024)**

240

241 All four glacial lakes exhibited statistically significant positive area trends over the 1992-2024 study period.  
242 Mann-Kendall test results confirm perfect monotonic increasing trends for every lake ( $\tau = 1$ ,  $Z = 3.65$ ,  $p = 2.63$   
243  $\times 10^{-4}$ ). Key results are summarized in Table 1.

244

245 **Table 1: Lake area statistics, uncertainty, Mann-Kendall results, and linear fit (1992-2024)**

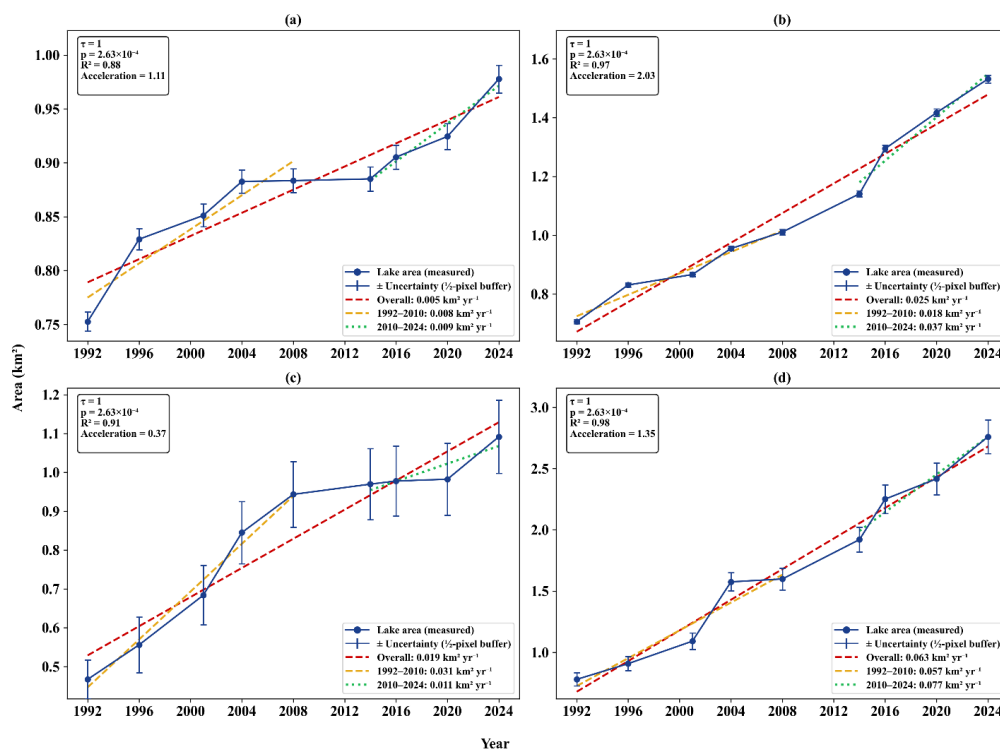
Lake	Area 1992 (km <sup>2</sup> ± uncertainty)	Area 2024 (km <sup>2</sup> ± uncertainty)	% Change	Sen Slope (km <sup>2</sup> yr <sup>-1</sup> )	Linear Slope (km <sup>2</sup> yr <sup>-1</sup> )	R <sup>2</sup>



Thulagi	$0.75 \pm 0.009$	$0.97 \pm 0.013$	$\approx 29.3\%$	0.005	0.0053	0.88
Lumding Tsho	$0.70 \pm 0.007$	$1.53 \pm 0.013$	$\approx 118.6\%$	0.025	0.025	0.97
Hongu 2	$0.46 \pm 0.05$	$1.09 \pm 0.094$	$\approx 137\%$	0.02	0.018	0.91
Lower Barun	$0.77 \pm 0.053$	$2.76 \pm 0.13$	$\approx 258\%$	0.063	0.063	0.98

246

247 Lower Barun showed the greatest absolute and proportional expansion, growing from  $0.77 \pm 0.053 \text{ km}^2$  to  $2.76 \pm$   
 248  $0.13 \text{ km}^2$ , a 258% increase over 32 years. Lumding Tsho exhibited persistent and highly linear upward growth,  
 249 reaching  $1.53 \text{ km}^2$  by 2024 ( $R^2 = 0.97$ ). Hongu 2 showed a characteristic step-change growth pattern: modest  
 250 expansion from 1992 to approximately 2005, followed by a sudden area increase between 2006 and 2007, then  
 251 slowest absolute growth but the highest linear fit ( $R^2 = 0.88$ ), indicating uninterrupted steady gradual expansion  
 252 throughout.



253

254 **Figure 2: Lake area time series (1992-2024) for (a) Thulagi, (b) Lumding Tsho, (c) Hongu 2, and (d)**

255 **Lower Barun, with Mann-Kendall confirmed trend lines and sub-period regression segments**



256

257 **4.2 Sub-Period Acceleration Analysis**

258

259 To assess whether lake expansion rates are accelerating or stabilising, linear regression was performed  
 260 separately for the 1992-2010 and 2010-2024 sub-periods. (Table 2).

261

262 **Table 2: Sub-period trend analysis comparing 1992-2010 and 2010-2024 lake expansion rates**

Lake	Slope 1992-2010 (km <sup>2</sup> yr <sup>-1</sup> )	Slope 2010-2024 (km <sup>2</sup> yr <sup>-1</sup> )	Acceleration factor	Interpretation
Thulagi	0.0079	0.0087	1.11	Modest acceleration
Lumding Tsho	0.018	0.037	2.03	Marked acceleration
Hongu 2	0.030	0.011	0.37	Post-event deceleration
Lower Barun	0.056	0.076	1.35	Marked acceleration

263

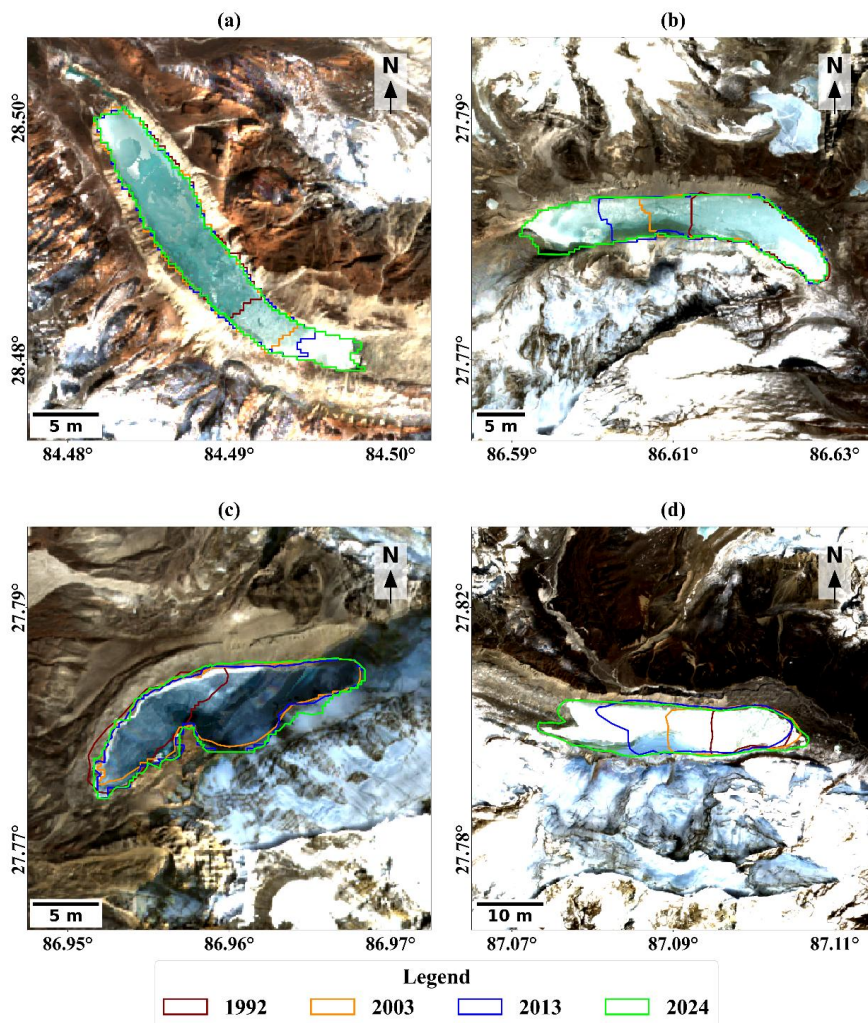
264 Lower Barun’s post-2010 expansion rate (0.077 km<sup>2</sup> yr<sup>-1</sup>) was more than double the pre-2010 rate (0.057 km<sup>2</sup> yr<sup>-1</sup>), an acceleration factor of 1.35. Hongu 2 showed a marked post-2010 deceleration (0.37), consistent with the  
 265 abrupt 2006-2007 growth event representing a discrete threshold crossing after which growth stabilized at a larger  
 266 extent. Thulagi showed a modest post-2010 acceleration of 11%, while Lumding Tsho showed the most  
 267 pronounced acceleration with a 2.03-fold increase post-2010.  
 268

269

270 **4.3 Spatial Dynamics of Lake Expansion**

271

272 Temporal mapping of lake boundaries confirms significant and directional growth in all four lakes. Spatial  
 273 analysis of boundary shift vectors reveals that all lakes expand preferentially in the upvalley direction, directly  
 274 towards and into the space progressively vacated by retreating glacier termini. In Lower Barun, the 2024 lake  
 275 boundary extends approximately 1.1 km further up-glacier compared to the 1992 extent. In Lumding Tsho, the  
 276 northern boundary facing the glacier terminus shows the greatest displacement, while the lateral moraine-  
 277 constrained margins are comparatively stable.



278

279 **Figure 3: Multi-temporal lake boundaries (1992, 2000, 2010, 2024) overlaid on 2024 Sentinel-2 imagery**

280 **for (a) Thulagi, (b) Lumding Tsho, (c) Hongu 2, and (d) Lower Barun**

281

#### 282 4.4 Estimated Volume Change

283

284 Empirical area-volume scaling using the Cook & Quincey (2015) relationship ( $V = 0.104 \times A^{1.42}$ ) provides

285 order-of-magnitude estimates of the water volume accumulated since 1992 (Table 3).

286

287 **Table 3: Estimated lake volumes using Cook & Quincey (2015) empirical scaling**

Lake	Area <sub>1992</sub> (km <sup>2</sup> )	V <sub>1992</sub> (× 10 <sup>6</sup> m <sup>3</sup> )	Area <sub>2024</sub> (km <sup>2</sup> )	V <sub>2024</sub> (× 10 <sup>6</sup> m <sup>3</sup> )	ΔV (× 10 <sup>6</sup> m <sup>3</sup> )
Thulagi	0.75	69.1	0.97	99.6	+30.5



Lumding Tsho	0.70	62.7	1.53	190.2	+127.5
Hongu 2	0.46	34.5	1.09	117.4	+82.9
Lower Barun	0.77	71.7	2.76	439.4	+367.7
Combined	2.68	238	6.35	846.6	+608.6

288

289 For lakes with field-measured volumes, the scaling equation overestimates the surveyed 2018 volume for Thulagi  
 290 (field:  $36.1 \times 10^6 \text{ m}^3$ ; scaling:  $\sim 80 \times 10^6 \text{ m}^3$ ). This overestimation is expected for Thulagi, which occupies a  
 291 relatively shallow, moraine-constrained basin. For Lower Barun (field:  $112.3 \times 10^6 \text{ m}^3$ ; in 2018), the 2024 scaling  
 292 estimate of  $439.4 \times 10^6 \text{ m}^3$  reflects the substantial post-survey growth and is broadly consistent with the observed  
 293 calving-driven volume increase documented by Gantayat et al. (2024). Volume estimates should be treated as  
 294 indicative order-of magnitude values. Nevertheless, the combined additional water volume across the four lakes  
 295 since 1992 ( $\sim 608.6 \times 10^6 \text{ m}^3$ ), equivalent to approximately 60 times the estimated flood volume of the destructive  
 296 1985 Dig Tsho GLOF (Vuichard & Zimmermann, 1987), underscores the scale of GLOF hazard potential these  
 297 systems collectively represent.

298

## 299 5 Discussion

300

### 301 5.1 Lake Expansion in the Context of regional Himalayan Trends

302

303 The statistically significant expansion of all four study lakes over 32 years is consistent with broad patterns  
 304 documented across the HKH region. Shugar et al. (2020) reported a 51% increase in global glacial lake area from  
 305 1990 to 2018, and studies focused specifically on Nepal document rapid lake proliferation in recent decades (Hu  
 306 et al., 2022; Kumar et al., 2025). The range of areal expansion rates across the four lakes, from Thulagi’s modest  
 307 29.3% growth to Lower Barun’s explosive 258% increase reflects the diversity of controls on proglacial lake  
 308 dynamics in the Himalaya, including glacier hypsometry, debris cover, moraine geometry, and basin topography  
 309 (Carrivick & Tweed, 2013; Rounce et al., 2017). Notably, all four lakes show monotonic trends of increasing area  
 310 with zero reversals over 9 timesteps between 1992 and 2024, a result that points to consistent, uninterrupted  
 311 physical forcing throughout the study period rather than episodic or oscillatory dynamics.

312

313 The post-2010 acceleration documented at Lower Barun (1.35 rate increase) is particularly major. Gantayat et al.  
 314 (2024) identified continuous glacier calving and increasing ice-cliff area at Lower Barun as primary drivers of its  
 315 accelerating expansion, with calving dynamics sensitive to lake thermal structure and glacier geometry. This  
 316 mechanism produces acceleration that outpaces what would be expected from atmospheric forcing alone, and  
 317 explains why the post-2010 rate change is more pronounced at Lower Barun than at the other three lakes.

318

### 319 5.2 Divergent Growth Patterns and Site-Specific Controls

320

321 The contrasting growth trajectories across the four lakes underscore the importance of site-specific analysis in  
 322 GLOF hazard assessment. Thulagi’s slow expansion reflects the narrow geometry of the Upper Marsyangdi basin  
 323 and the relatively smaller, less dynamic nature of the Thulagi glacier. Haritashya et al. (2018) documented a



324 gradual increase from 0.4 km<sup>2</sup> in the early 1970s to 0.9 km<sup>2</sup> by 2017, consistent with our finding of 0.97 km<sup>2</sup> by  
325 2024, confirming continuity of this gradual trend over five decades.

326

327 Hongu 2's step-change growth between 2006 and 2007 suggests a threshold event, likely an ice-calving episode,  
328 subaqueous moraine adjustment, or a sudden meltwater influx, that abruptly enlarged the lake before stabilization.  
329 The post-2007 deceleration factor of 0.37 indicates that the lake is now expanding towards a new, constrained  
330 equilibrium after the discrete threshold-crossing event consumed the available accommodation space within the  
331 existing moraine basin. This pattern highlights how gradual climate-driven glacier retreat can produce punctuated,  
332 threshold-driven lake responses when geomorphological boundaries are crossed (Carrivick & Tweed, 2013).

333

334 Lumding Tsho's steady, uninterrupted expansion rate, with no sign of deceleration, is consistent with its hazardous  
335 configuration described by Bajracharya et al. (2020): a lake pinned between steep slopes and hanging glacier ice,  
336 fed by continuous meltwater, with a relatively short and potentially vulnerable moraine dam. An accelerating  
337 Sen's slope of 0.025 km<sup>2</sup> yr<sup>-1</sup> and a post-2010 acceleration factor of 2.03 indicates that Lumding Tsho expansion  
338 is gathering pace, with the rate of growth increasing through the study period.

339

### 340 **5.3 Volume Implications for GLOF Hazard**

341

342 The estimated additional water volume accumulated across the four lakes since 1992 approaches  $608.6 \times 10^6$  m<sup>3</sup>,  
343 more than tripling their baseline combined volume. The individual volume increase at Lower Barun alone ( $\sim 367.7$   
344  $\times 10^6$  m<sup>3</sup>) represents a hazard of exceptional scale: the 1985 Dig Tsho GLOF, which caused catastrophic damage  
345 to downstream infrastructure, villages, and the Manche Small Hydro project, involved an estimated flood volume  
346 of only  $5\text{--}10 \times 10^6$  m<sup>3</sup> (Richardson & Reynolds, 2000). Even allowing for inherent uncertainties in the A-V scaling,  
347 the order-of-magnitude increase in impounded water at Lower Barun represents a fundamentally different hazard  
348 class from documented events in Nepal. The Lumding Tsho volume increase ( $+127 \times 10^6$  m<sup>3</sup>), concentrated behind  
349 a short moraine dam adjacent to hanging ice as described by Bajracharya et al. (2020), similarly represents an  
350 extreme potential hazard given the dam's structural characteristics.

351

352 These volume estimates reinforce the scientific evidence and provide the quantitative water-volume context that  
353 hazard exposure modelling requires. Future work integrating these volume estimates with hydrodynamic GLOF  
354 routing models, as applied by Maskey et al. (2020) for Thulagi and Lower Barun, should update the routing  
355 analyses with the substantially larger 2024 lake volumes presented here.

356

### 357 **5.4 Methodological Limitations**

358

359 Several methodological limitations apply to this study. First, NDWI-based lake delineation at 30 m Landsat  
360 resolution carries inherent uncertainty, quantified here using the standard half-pixel buffer method. The perimeter-  
361 based uncertainty values in Table 1 represent pixel-level geometric uncertainty; additional uncertainty may arise  
362 from inter-annual variation in water surface levels due to seasonal drawdown or infill, which is partially controlled  
363 by restricting analysis to post-monsoon (October–November) composites when lake levels are near their seasonal  
364 maximum.



365

366 Second, the 2012-2013 data gap due to Landsat 7 SLC-off failure required substitution of 2014 imagery,  
367 introducing a slightly uneven temporal spacing. This does not affect the monotonic trend result but should be  
368 noted in interpreting sub-period regression coefficients.

369

370 Third, the area-volume scaling of Cook & Quincey (2015) carries substantial uncertainty for individual lakes,  
371 particularly those in highly over-deepened basins. Field-measured volumes for Thulagi and Lower Barun confirm  
372 the scaling equation overestimates shallow, confined basins (Thulagi), while performing more consistently for  
373 deep, calving-fed systems (Lower Barun). Volume estimates should therefore be treated as order-of-magnitude  
374 indicators, and high-resolution bathymetric surveys are recommended to refine these values ahead of detailed  
375 GLOF routing modelling.

376

377 Fourth, this study does not include quantitative glacier retreat mapping. Qualitative evidence for the casual link  
378 between glacier retreat and lake expansion is supported by published literature (Byers et al., 2013; Gantayat et al.,  
379 2024; Haritashya et al., 2018; Maskey et al., 2020), and the spatial dynamics of up-valley lake boundary expansion  
380 (Section 4.3) are consistent with glacier-driven expansion. Future work should incorporate glacier area change  
381 mapping, using field-validated glacier outlines rather than indices based on satellite imagery alone, which are  
382 unreliable for debris-covered glaciers that constitute a large fraction of total ice area at these sites.

383

## 384 **6 Conclusion**

385

386 This study presents the most comprehensive multi-decadal analysis to date of the four potentially dangerous  
387 glacial lakes in central-eastern Nepal, integrating lake area change, uncertainty quantification, volume estimation,  
388 and sub-period acceleration analysis within a unified remote sensing and statistical framework spanning 1992 to  
389 2024.

390

391 All four lakes exhibit statistically significant monotonic expansion confirmed by Mann-Kendall trend tests ( $\tau =$   
392  $1, p = 2.63 \times 10^{-4}$ ). Lower Barun has undergone the most dramatic transformation: +258% areal growth, a post-  
393 2010 acceleration factor of 1.35, and an estimated additional impounded water volume of  $+367.7 \times 10^6 \text{ m}^3$ .  
394 Lumding Tsho maintains an undiminished linear expansion rate (Sen's slope =  $0.025 \text{ km}^2 \text{ yr}^{-1}$ ) with no sign of  
395 geometric constraint, representing the most persistently growing hazard among the four lakes. Hongu 2  
396 experienced a discrete threshold-crossing growth event around 2006-2007 followed by slower growth at around  
397 0.37 of the previous rates. Thulagi continues steady expansion with a 1.11 post-2010 modest acceleration. The  
398 combined estimated volume increases across all four lakes since 1992 approaches  $608.6 \times 10^6 \text{ m}^3$ .

399

400 These findings collectively validate the scientific basis to support the following specific prioritisations: (i) urgent  
401 lake lowering at Lower Barun given its explosive post-2010 acceleration and exceptional volume increase; (ii)  
402 sustained monitoring of Lumding Tsho given its undiminished linear expansion and vulnerable moraine dam  
403 configurations; (iii) continued area monitoring of Thulagi with attention to its structurally sensitive ice-cored  
404 moraine dam; and (iv) trigger-event focused early warning monitoring of Hongu 2, given its demonstrated  
405 capacity for episodic, threshold-driven expansion.



406

407 Future work should incorporate high-resolution bathymetric surveys to refine volume estimates, field-validated  
408 glacier outline mapping using SAR and thermal infrared methods to quantify debris-covered ice loss, and updated  
409 cascade GLOF hydrodynamic modelling using the current 2024 lake volumes presented here.

410

#### 411 **Code and data availability**

412

413 The Google Earth Engine code and Python analysis used in this study were developed entirely by authors. Landsat  
414 imagery was accessed via Google Earth Engine (<https://earthengine.google.com>) and Sentinel-2 image was  
415 accessed via the Copernicus Open Access Hub (<https://copernicus.eu>), both of which are publicly available.

416

#### 417 **Author Contributions**

418

419 AG conceptualized the study, designed the methodology, developed all Google Earth Engine and Python analysis  
420 codes, performed the data processing, conducted the statistical analysis, and led the writing manuscript. SM, TB,  
421 RK, and AD contributed to manuscript preparation, writing, and editing. KA and DP provided scientific review,  
422 supervision, and critical revision of the manuscript. All authors reviewed and approved the final version.

423

#### 424 **Competing Interests**

425

426 The authors declare that they have no conflict of interest.

427

#### 428 **Financial support**

429

430 This research received no specific grant from any funding agency in the public, commercial, or non-profit sectors.

431

#### 432 **References**

433

434 Bajracharya, S. R., Maharjan, S. B., Shrestha, F., Guo, W., Liu, S., Immerzeel, W., & Shrestha, B. (2015). The  
435 glaciers of the Hindu Kush Himalayas: current status and observed changes from the 1980s to 2010.  
436 *International Journal of Water Resources Development*, 31(2), 161–173.  
437 <https://doi.org/10.1080/07900627.2015.1005731>

438 Bajracharya, S. R., Maharjan, S. B., Shrestha, F., Sherpa, T. C., Wagle, N., & Shrestha A.B. (2020). *Inventory*  
439 *of glacial lakes and identification of potentially dangerous glacial lakes in the Koshi, Gandaki, and*  
440 *Karnali river basins of Nepal, the Tibet autonomous region of China, and India*. International Centre for  
441 Integrated Mountain Development and United Nations Development Programme.

442 Bocchiola, D., Manara, M., & Mereu, R. (2020). Hydropower potential of run of river schemes in the himalayas  
443 under climate change: A case study in the dudh koshi basin of Nepal. *Water (Switzerland)*, 12(9).  
444 <https://doi.org/10.3390/W12092625>

445 Bookhagen, B., & Burbank, D. W. (2010). Toward a complete Himalayan hydrological budget: Spatiotemporal  
446 distribution of snowmelt and rainfall and their impact on river discharge. *Journal of Geophysical*  
447 *Research: Earth Surface*, 115(3). <https://doi.org/10.1029/2009JF001426>



- 448 Byers, A. C., McKinney, D. C., Somos-Valenzuela, M., Watanabe, T., & Lamsal, D. (2013). Glacial lakes of the  
449 Hinku and Hongu valleys, Makalu Barun National Park and Buffer Zone, Nepal. *Natural Hazards*, 69(1),  
450 115–139. <https://doi.org/10.1007/s11069-013-0689-8>
- 451 Carrivick, J. L., & Tweed, F. S. (2013). Proglacial lakes: character, behaviour and geological importance.  
452 *Quaternary Science Reviews*, 78, 34–52. <https://doi.org/10.1016/J.QUASCIREV.2013.07.028>
- 453 Chen, H., Liang, Q., Zhao, J., & Maharjan, S. B. (2024). *Assessing national exposure and impact to glacial lake*  
454 *outburst floods considering uncertainty under data sparsity*. <https://doi.org/10.5194/hess-2023-260>
- 455 Chen, H., Liang, Q., Zhao, J., & Maharjan, S. B. (2025). Assessing national exposure to and impact of glacial  
456 lake outburst floods considering uncertainty under data sparsity. *Hydrology and Earth System Sciences*,  
457 29(3), 733–752. <https://doi.org/10.5194/hess-29-733-2025>
- 458 Cook, S. J., & Quincey, D. J. (2015). Estimating the volume of Alpine glacial lakes. *Earth Surface Dynamics*,  
459 3(4), 559–575. <https://doi.org/10.5194/esurf-3-559-2015>
- 460 Duan, H., Yao, X., Zhang, Y., Jin, H., Wang, Q., Du, Z., Hu, J., Wang, B., & Wang, Q. (2023). Lake volume  
461 and potential hazards of moraine-dammed glacial lakes - A case study of Bienong Co, southeastern  
462 Tibetan Plateau. *Cryosphere*, 17(2), 591–616. <https://doi.org/10.5194/tc-17-591-2023>
- 463 Fujita, K., Sakai, A., Nuimura, T., Yamaguchi, S., & Sharma, R. R. (2009). Recent changes in Imja Glacial  
464 Lake and its damming moraine in the Nepal Himalaya revealed by in situ surveys and multi-temporal  
465 ASTER imagery. *Environmental Research Letters*, 4(4). <https://doi.org/10.1088/1748-9326/4/4/045205>
- 466 Gantayat, P., Sattar, A., Haritashya, U. K., Ramsankaran, R. A. A. J., & Kargel, J. S. (2024). Evolution of the  
467 Lower Barun lake and its exposure to potential mass movement slopes in the Nepal Himalaya. *Science of*  
468 *the Total Environment*, 949. <https://doi.org/10.1016/j.scitotenv.2024.175028>
- 469 Gu, Y., Brown, J. F., Verdin, J. P., Wardlow, B., Gu, Y., Brown, J. F., Verdin, J. P., & Wardlow, B. (2007). A  
470 five-year analysis of MODIS NDVI and NDWI for grassland drought assessment over the central Great  
471 Plains of the United States. *Geophysical Research Letters*, 34(6). <https://doi.org/10.1029/2006GL029127>
- 472 Gurung, N., Thakuri, S., Chauhan, R., Ghimire, N. P., & Ghimire, M. (2021). Dynamics of Lower-Barun  
473 Glacier and Glacial Lake and its GLOF Susceptibility Using Geospatial Analysis and Modelling.  
474 *Jalawaayu*, 1(2), 57–77. <https://doi.org/10.3126/jalawaayu.v1i2.41012>
- 475 Haritashya, U. K., Kargel, J. S., Shugar, D. H., Leonard, G. J., Stratman, K., Watson, C. S., Shean, D.,  
476 Harrison, S., Mandli, K. T., & Regmi, D. (2018). Evolution and controls of large glacial lakes in the Nepal  
477 Himalaya. *Remote Sensing*, 10(5). <https://doi.org/10.3390/rs10050798>
- 478 Hermosilla, T., Francini, S., Nicolau, A. P., Wulder, M. A., White, J. C., Coops, N. C., & Chirici, G. (2023).  
479 Clouds and Image Compositing. *Cloud-Based Remote Sensing with Google Earth Engine: Fundamentals*  
480 *and Applications*, 279–302. [https://doi.org/10.1007/978-3-031-26588-4\\_15/FIGURES/12](https://doi.org/10.1007/978-3-031-26588-4_15/FIGURES/12)
- 481 Hu, J., Yao, X., Duan, H., Zhang, Y., Wang, Y., & Wu, T. (2022). Temporal and Spatial Changes and GLOF  
482 Susceptibility Assessment of Glacial Lakes in Nepal from 2000 to 2020. *Remote Sensing*, 14(19).  
483 <https://doi.org/10.3390/rs14195034>
- 484 Huggel, C., Käab, A., Haeberli, W., Teyssie, P., & Paul, F. (2002). Remote sensing based assessment of  
485 hazards from glacier lake outbursts: A case study in the Swiss Alps. *Canadian Geotechnical Journal*,  
486 39(2), 316–330. <https://doi.org/10.1139/t01-099>
- 487 ICIMOD. (2011). *Glacial Lakes and Glacial Lake Outburst Floods in Nepal*.
- 488 ICIMOD. (2023). Water, ice, society, and ecosystems in the Hindu Kush Himalaya: An outlook. In R. Chettri,  
489 N. Adve, C. Wickramagamage, & K. Shrestha (Eds.), *Water, ice, society, and ecosystems in the Hindu*  
490 *Kush Himalaya: An outlook*. ICIMOD. <https://doi.org/10.53055/icimod.1028>
- 491 Ives, J. D., Shrestha, R. B., & Mool, P. K. (2010). *Formation of Glacial Lakes in the Hindu Kush-Himalayas*  
492 *and GLOF Risk Assessment*.



- 493 Jin, H., Fang, S., & Chen, C. (2023). Mapping of the Spatial Scope and Water Quality of Surface Water Based  
494 on the Google Earth Engine Cloud Platform and Landsat Time Series. *Remote Sensing*, 15(20).  
495 <https://doi.org/10.3390/rs15204986>
- 496 Kendall, & George, M. (1990). *Rank correlation methods*. Internet Archive.  
497 <https://archive.org/details/rankcorrelationm0000unse/page/n1/mode/2up>
- 498 Komori, J. (2006). Glacial Lake Expansion and Present Situation in Hinku and Hongu Regions, Eastern Nepal  
499 and Bhutan Himalaya. *Journal of Geography (Chigaku Zasshi)*, 115(4), 531–535.  
500 [https://doi.org/10.5026/jgeography.115.4\\_531](https://doi.org/10.5026/jgeography.115.4_531)
- 501 Kumar, A., Mal, S., Schickhoff, U., & Dimri, A. P. (2025). Basin-scale spatio-temporal development of glacial  
502 lakes in the Hindukush-Karakoram-Himalayas. *Global and Planetary Change*, 245, 104656.  
503 <https://doi.org/10.1016/J.GLOPLACHA.2024.104656>
- 504 Lee, H., & Romero, J. (2023). Climate Change 2023 Synthesis Report IPCC, 2023: Sections. In: Climate  
505 Change 2023: Synthesis Report. Contribution of Working Groups I, II and III to the Sixth Assessment  
506 Report of the Intergovernmental Panel on Climate Change [Core Writing Team. *IPCC*, 35–115.  
507 <https://doi.org/10.59327/IPCC/AR6-9789291691647>
- 508 Mann, H. B. (1945). Nonparametric Tests Against Trend. *Econometrica*, 13(3), 245.  
509 <https://doi.org/10.2307/1907187>
- 510 Maskey, S., Kayastha, R. B., & Kayastha, R. (2020). Glacial Lakes Outburst Floods (GLOFs) modelling of  
511 Thulagi and Lower Barun Glacial Lakes of Nepalese Himalaya. *Progress in Disaster Science*, 7.  
512 <https://doi.org/10.1016/j.pdisas.2020.100106>
- 513 McFeeters, S. K. (2013). Using the Normalized Difference Water Index (NDWI) within a Geographic  
514 Information System to Detect Swimming Pools for Mosquito Abatement: A Practical Approach. *Remote  
515 Sensing 2013*, Vol. 5, Pages 3544–3561, 5(7), 3544–3561. <https://doi.org/10.3390/RS5073544>
- 516 Mudbhari, D., Kansal, M. L., & Kalura, P. (2022). Impact of climate change on water availability in Marsyangdi  
517 river basin, Nepal. *Quarterly Journal of the Royal Meteorological Society*, 148(744), 1407–1423.  
518 <https://doi.org/10.1002/QJ.4267>
- 519 Nepal, S. (2016). Impacts of climate change on the hydrological regime of the Koshi river basin in the  
520 Himalayan region. *Journal of Hydro-Environment Research*, 10, 76–89.  
521 <https://doi.org/10.1016/j.jher.2015.12.001>
- 522 Neupane, R. P., White, J. D., & Alexander, S. E. (2015). Projected hydrologic changes in monsoon-dominated  
523 Himalaya Mountain basins with changing climate and deforestation. *Journal of Hydrology*, 525, 216–230.  
524 <https://doi.org/10.1016/j.jhydrol.2015.03.048>
- 525 Paul, F., Barrand, N. E., Baumann, S., Berthier, E., Bolch, T., Casey, K., Frey, H., Joshi, S. P., Konovalov, V.,  
526 Le Bris, R., Mölg, N., Nosenko, G., Nuth, C., Pope, A., Racoviteanu, A., Rastner, P., Raup, B., Scharrer,  
527 K., Steffen, S., & Winsvold, S. (2013). On the accuracy of glacier outlines derived from remote-sensing  
528 data. *Annals of Glaciology*, 54(63), 171–182. <https://doi.org/10.3189/2013AoG63A296>
- 529 Pepin, N. C., Amone, E., Gobiet, A., Haslinger, K., Kotlarski, S., Notarnicola, C., Palazzi, E., Seibert, P.,  
530 Serafin, S., Schöner, W., Terzagio, S., Thornton, J. M., Vuille, M., & Adler, C. (2022). Climate Changes  
531 and Their Elevational Patterns in the Mountains of the World. In *Reviews of Geophysics* (Vol. 60, Number  
532 1). John Wiley and Sons Inc. <https://doi.org/10.1029/2020RG000730>
- 533 Richardson, S. D., & Reynolds, J. M. (2000). An overview of glacial hazards in the Himalayas. *Quaternary  
534 International*, 65–66, 31–47. [https://doi.org/10.1016/S1040-6182\(99\)00035-X](https://doi.org/10.1016/S1040-6182(99)00035-X)
- 535 Rounce, D. R., Watson, C. S., & McKinney, D. C. (2017). Identification of hazard and risk for glacial lakes in  
536 the Nepal Himalaya using satellite imagery from 2000–2015. *Remote Sensing*, 9(7).  
537 <https://doi.org/10.3390/rs9070654>
- 538 Scaramuzza, P., Micijevic, E., & Chander, G. (2004). *SLC Gap-Fill Methodology*.



- 539 Sen, P. K. (1968). Estimates of the Regression Coefficient Based on Kendall's Tau. *Journal of the American*  
540 *Statistical Association*, 63(324), 1379–1389. <https://doi.org/10.1080/01621459.1968.10480934>
- 541 Shugar, D. H., Burr, A., Haritashya, U. K., Kargel, J. S., Watson, C. S., Kennedy, M. C., Bevington, A. R.,  
542 Betts, R. A., Harrison, S., & Stratman, K. (2020). Rapid worldwide growth of glacial lakes since 1990.  
543 *Nature Climate Change* 2020 10:10, 10(10), 939–945. <https://doi.org/10.1038/s41558-020-0855-4>
- 544 Sigdel, K. P., Ghimire, N. P., Pandeya, B., & Dawadi, B. (2022). Historical and Projected Variations of  
545 Precipitation and Temperature and Their Extremes in Relation to Climatic Indices over the Gandaki River  
546 Basin, Central Himalaya. *Atmosphere*, 13(11). <https://doi.org/10.3390/atmos13111866>
- 547 UNDP. (2025). *Green Climate Fund approves \$36.1 million to help Nepal protect lives and livelihoods from*  
548 *glacial flood risks | United Nations Development Programme*. [https://www.undp.org/nepal/press-](https://www.undp.org/nepal/press-releases/green-climate-fund-approves-361-million-help-nepal-protect-lives-and-livelihoods-glacial-flood-risks)  
549 [releases/green-climate-fund-approves-361-million-help-nepal-protect-lives-and-livelihoods-glacial-flood-](https://www.undp.org/nepal/press-releases/green-climate-fund-approves-361-million-help-nepal-protect-lives-and-livelihoods-glacial-flood-risks)  
550 [risks](https://www.undp.org/nepal/press-releases/green-climate-fund-approves-361-million-help-nepal-protect-lives-and-livelihoods-glacial-flood-risks)
- 551 Vuichard, D., & Zimmermann, M. (1987). The 1985 Catastrophic Drainage of a Moraine-Dammed Lake,  
552 Khumbu Himal, Nepal: Cause and Consequences. *Source: Mountain Research and Development*, 7(2),  
553 91–110. <https://doi.org/10.7892/boris.72507>
- 554 Wangchuk, S., & Bolch, T. (2020). Mapping of glacial lakes using Sentinel-1 and Sentinel-2 data and a random  
555 forest classifier: Strengths and challenges. *Science of Remote Sensing*, 2,  
556 <https://doi.org/10.1016/j.srs.2020.100008>
- 557 Williams, D. L., Goward Samuel, & Arvidson, T. (2006). Landsat: Yesterday, Today, and Tomorrow.  
558 *Photogrammetric Engineering & Remote Sensing*, 72(10), 1171–1178. 10.14358/PERS.72.10.1171
- 559 Yue, S., Pilon, P., Phinney, B., & Cavadias, G. (2002). The influence of autocorrelation on the ability to detect  
560 trend in hydrological series. *Hydrological Processes*, 16(9), 1807–1829. <https://doi.org/10.1002/hyp.1095>
- 561
- 562